

Master Thesis

Multi Phase Modelling an Finite Element Implementation of Steel Heat Treatment

conducted at

Institute of Mechanics,
Department of Mechanical Engineering,
TU Dortmund

by

Philipp Scherm

on

March 1, 2023

Supervisors:

Prof. Dr.-Ing. habil. Andreas Menzel
Markus Schewe, M. Sc.

Eidesstattliche Versicherung (Affidavit)

Name, Vorname
(Last name, first name)

Matrikelnr.
(Enrollment number)

Ich versichere hiermit an Eides statt, dass ich die vorliegende Bachelorarbeit/Masterarbeit* mit dem folgenden Titel selbstständig und ohne unzulässige fremde Hilfe erbracht habe. Ich habe keine anderen als die angegebenen Quellen und Hilfsmittel benutzt sowie wörtliche und sinngemäße Zitate kenntlich gemacht. Die Arbeit hat in gleicher oder ähnlicher Form noch keiner Prüfungsbehörde vorgelegen.

I declare in lieu of oath that I have completed the present Bachelor's/Master's* thesis with the following title independently and without any unauthorized assistance. I have not used any other sources or aids than the ones listed and have documented quotations and paraphrases as such. The thesis in its current or similar version has not been submitted to an auditing institution.

Titel der Bachelor-/Masterarbeit*:
(Title of the Bachelor's/ Master's* thesis):

*Nichtzutreffendes bitte streichen
(Please choose the appropriate)

Ort, Datum
(Place, date)

Unterschrift
(Signature)

Belehrung:

Wer vorsätzlich gegen eine die Täuschung über Prüfungsleistungen betreffende Regelung einer Hochschulprüfungsordnung verstößt, handelt ordnungswidrig. Die Ordnungswidrigkeit kann mit einer Geldbuße von bis zu 50.000,00 € geahndet werden. Zuständige Verwaltungsbehörde für die Verfolgung und Ahndung von Ordnungswidrigkeiten ist der Kanzler/die Kanzlerin der Technischen Universität Dortmund. Im Falle eines mehrfachen oder sonstigen schwerwiegenden Täuschungsversuches kann der Prüfling zudem exmatrikuliert werden. (§ 63 Abs. 5 Hochschulgesetz - HG -).

Die Abgabe einer falschen Versicherung an Eides statt wird mit Freiheitsstrafe bis zu 3 Jahren oder mit Geldstrafe bestraft.

Die Technische Universität Dortmund wird ggf. elektronische Vergleichswerkzeuge (wie z.B. die Software „turnitin“) zur Überprüfung von Ordnungswidrigkeiten in Prüfungsverfahren nutzen.

Die oben stehende Belehrung habe ich zur Kenntnis genommen:

Official notification:

Any person who intentionally breaches any regulation of university examination regulations relating to deception in examination performance is acting improperly. This offense can be punished with a fine of up to €50,000.00. The competent administrative authority for the pursuit and prosecution of offenses of this type is the chancellor of TU Dortmund University. In the case of multiple or other serious attempts at deception, the examinee can also be unenrolled, section 63, subsection 5 of the North Rhine-Westphalia Higher Education Act (*Hochschulgesetz*).

The submission of a false affidavit will be punished with a prison sentence of up to three years or a fine.

As may be necessary, TU Dortmund will make use of electronic plagiarism-prevention tools (e.g. the "turnitin" service) in order to monitor violations during the examination procedures.

I have taken note of the above official notification:**

Ort, Datum
(Place, date)

Unterschrift
(Signature)

****Please be aware that solely the German version of the affidavit ("Eidesstattliche Versicherung") for the Bachelor's/ Master's thesis is the official and legally binding version.**

Contents

1	Introduction	3
2	Model/Theoretical Framework/Method	5
2.1	Metallurgy	5
2.2	Phase Transformations	6
2.2.1	Involved Phases	10
2.2.2	phenomenological models	10
2.3	Thermal Problem	11
2.4	mechanical	11
3	Algorithmic implementation	13
3.1	Implementation in Abaqus	14
3.2	Avrami+addi	15
3.3	Parametrisation of TTT-diagrams	17

Chapter 1

Introduction

Heat treatment of metals as a way of altering its properties and microstructure is a process known for millennia. For many millennia heat treatment of metals has been an important part of industrial development. The ancient egyptians used annealing to

The heat treatment process of steel usually involves vigorously heating the metal and throwing it into cold water. A later less vigorous reheating is optional. *Maybe spare this for the presentation*

Define heat treatment

talk about history islamic, egypt, india, china, 9000 years bc

Chapter 2

Model/Theoretical Framework/Method

Heat treatment problems require the solution of three problems. Heat transfer, mechanical material response and phase transformation are coupled by their physical interactions.

2.1 Metallurgy

Heat treatment of steel aims to alter the microstructure in

Influence on the decomposition of austenite by the cooling rate and path

The German standard [DIN EN 10020 \[2000\]](#) defines steel in the most common form to be iron with a carbon content below 2%. Depending on the microstructure different phases are distinguished. They are characterized by their chemical composition, crystal lattice and shape. These characteristics influence the macroscopical properties exhibited by steel like strength, toughness, hardness and ductility. In a heat treatment process the microstructure and the properties can be altered. Here three different phases are of interest, austenite, pearlite, bainite and martensite. When steel is heated and held at a sufficient temperature and sufficient time it consists of stable and solid austenite. Austenite has a face-centered cubic lattice (γ -iron) with the an iron atom on every corner and at the center of each face. The carbon is dissolved in the interstitial spaces between the iron atoms. Austenite is the starting point of the modelled quenching process.

Martensite was discovered by Floris Osmond and named after Adolf Martens in [Osmond \[1904\]](#). It forms when austenite is quenched with a high cooling rate so that the diffusion of carbon out of the lattice is suppressed. Martensite exhibits a body-centered tetragonal structure and is supersaturated with carbon. The stretch from a cubic austenite structure to tetragonal martensite causes shear strains of a magnitude of 0.26, see [Bhadeshia \[2001\]](#), and dislocations that lead to high hardness of martensite. From martensitic steel a Brinell hardness of 700 can be achieved while the maximum of a pearlitic structure is approximately 400 Brinell, c.f. [Paxton and Redmond \[2007\]](#).

In [Cohen et al. \[1992\]](#) the martensite transformation is described as being of displacive nature, accompanied by a change in the crystal lattice. In steel it is athermal. There is no thermal activation, e. g. incubation time and no time dependence.

The transformation starts at the martensite start temperature M_S and is driven by cooling until the martensite finish temperature M_F is reached. The transformation is only driven by cooling and not by the time spent below M_S . If there is no further cooling the transformation stops. It is possible for a material cooled to room temperature to retain austenite if the M_F temperature is below room temperature.

In iron-alloys without carbon martensite transformation occurs isothermally.

When not quenched quickly enough to suppress it, diffusion of carbon occurs below the temperature A_3 . With decreasing temperature, the carbon-solubility of austenite drops and carbon diffuses out of the lattice. The carbon-depleted structure turns into ferrite which is almost pure iron with a body-centered cubic lattice (α). The locally carbon-enriched neighbouring structure turns into perlite. Perlite is a mixture of 87.5 wt% ferrite and 12.5 wt% carbide in lamellar structure that forms below the temperature A_1 . By the diffusion of carbon the structure is alternately locally carbon-enriched and depleted. In the depleted parts ferrite forms while the enriched structure turns into cementite. Cementite is a chemical compound of iron and steel Fe_3C . The lamellae structure is similar to that of mother-of-pearl which gives the steel phase its name.

While there are views that bainite is formed in a reconstructive way [Bhadeshia and Christian \[1990\]](#), in this thesis the bainite formation is regarded as displacive [Bhadeshia \[2019\]](#). Below a temperature of about 580°C reconstructive transformation is virtually non-existent because iron and alloying atoms are virtually immobile while carbon still solutes. [Christian \[1990\]](#) - bainite start temperature

Bainite is formed below the bainite start temperature B_S when the matrix atoms of the lattice are virtually immobile while the carbon atoms are still in solution. Upper bainite above M_S lower bainite below it.

Differentiation of the transformations in reproductive-displacive and athermal-isothermal [Bhadeshia and Christian \[1990\]](#)

2.2 Phase Transformations

Within this work two different kind of phase transformations are treated. Martensite transformation is athermal without thermal activation while the transformation into bainite is diffusion controlled. The bainite transformation is time dependent while martensite transformation is only driven by cooling, c.f. [Totten \[2007\]](#).

For the microstructural problem two different widely accepted (sources!!!) phenomenological models are used.

The martensite transformation relies on the Koistinen-Marburger model established by [Koistinen and Marburger \[1959\]](#). It describes the transformation using the following equation

As dargelegt in the previous chapter athermal and diffusion-controlled phase transformations are treated in this thesis. In athermal transformations there is no thermal activation, e. g. incubation time and no time dependence. The transformation is purely driven by cooling. If there is no further cooling the transformation stops. The transformation from austenite to martensite is regarded as being athermal. Its modelling relies on the Koistinen-Marburger model established in [Koistinen and Marburger \[1959\]](#). It describes the evolution of the volume fraction of

martensite β_M that is also depicted in fig. 2.1 using the following equation

$$\beta_M = 1 - e^{-k(M_S - T)} \quad . \quad (2.1)$$

The parameter k is material specific and describes the speed of the transformation. The martensite starting temperature M_S depends on the material and the other factors as the local carbon content that can be influenced by other phase transformations ??.. It determines the temperature at which the transformation starts. The transformation is regarded as complete when the martensitic volume fraction reaches 99%. The martensite finish temperature M_F can be calculated by rearranging 2.1 and inserting $\beta_M = 99\%$.

The rate of the martensite transformation can be described by

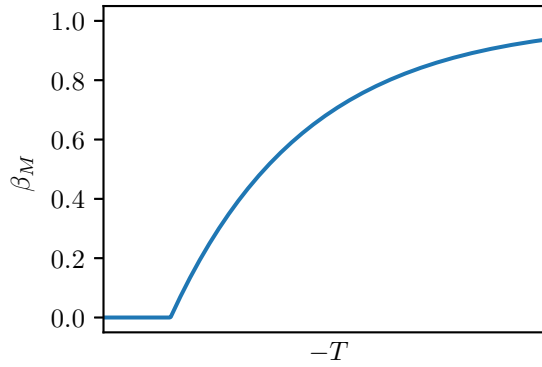


Figure 2.1: Development of the martensite volume fraction under cooling.

$$\dot{\beta}_M = -e^{-k[M_S - T]} k \dot{T} = \left[1 - e^{-k[M_S - T]} - 1 \right] k \dot{T} = -[1 - \beta_M] k \dot{T} \quad . \quad (2.2)$$

While this equation is valid when only considering the transformation from austenite to martensite it can be generalized for the usage with more phase transformations by interpreting the term $1 - \beta_M$ as the remaining austenite β_A available for transformation. This yields the following rate for the evolution of the martensitic phase

$$\dot{\beta}_M = -\beta_A k \dot{T} \quad . \quad (2.3)$$

The other transformation considered in this thesis is regarded as diffusion-controlled with thermal activation. There is a time-dependence in these transformations and they do continue isothermally when the cooling is stopped ??.. The transformation from austenite to bainite falls into this category. Schlecht.

Diffusional processes and transformations are often modelled using the... The equation used to describe this transformation is the JMAK law developed by Johnson, Mehl, Avrami and Kolmogorov (Avrami, 1940; Cahn, 1956) which is only valid for isothermal transformations. The JMAK law

$$\beta_B = \hat{\beta}_B [1 - e^{-b_B (t^{N_B})}] \quad (2.4)$$

can be used for various diffusional transformations and other time dependent processes. ?.. Here it is used to model the development of the volume fraction of bainite β_B where $\hat{\beta}_B$ is the maximal amount of bainite reached in the transformation. Irgendwas mit $\hat{\beta}_B = \beta_A + \beta_B$

with the maximal volume fraction of bainite $\hat{\beta}_B = \beta_A + \beta_B$ that can be reached if all austenite and the yields sigmoidal shapes seen in fig. 2.3 with a slow start and a slow finish of the transformation but a high rate in between. The parameters

$$N_B(T) = \frac{6.1273}{\ln\left(\frac{t_B^f}{t_B^s}\right)} \quad \text{and} \quad b_B(T) = \frac{0.01005}{(t_B^s)^{N_B(T)}} \quad (2.5)$$

are derived using the starting and finishing time t_B^s and t_B^f for the diffusive transformation. Those are defined at volume fraction of 1% and 99% of the target phase. The parameters are temperature dependent and can be determined from experimental TTT diagrams (Diss Yu 1977 oder so).

The time derivation of the JMAK law eq. 3.13 yields the rate equation for isothermal cooling

$$\dot{\beta}_B = \hat{\beta}_B b_B N_B t^{(N_B-1)} [1 - \beta_B] \quad (2.6)$$

As the JMAK law—and TTT-diagrams from which the parameters are derived—is only valid for isothermal transformations it has to be adapted to depict a cooling process.

In Scheil [1935] a theory of the additivity of fractional nucleation is proposed to predict the start of the transformation from austenite during cooling. The so-called ‘additivity rule’ states that transformation starts when the fractions of nucleation $\frac{\Delta t_i}{\tau(T_i)}$ accumulated during the cooling reaches unity

$$\int_{T_0}^{T_x} \frac{dt}{\tau(T)} = 1 \quad (2.7)$$

T_0 is an equilibrium temperature at which no nucleation happens, T_x is the temperature at which the transformation starts when following an anisothermal temperature path and $\tau(T)$ is the incubation time after that transformation starts for an isothermal temperature path. This means for a discretized calculation that the transformation starts when the fractions of nucleation at every time increment $\frac{\Delta t_i}{\tau(T_i)}$ amassed during the cooling reaches unity as follows

$$\sum \frac{\Delta t_i}{\tau(T_i)} = 1 \quad (2.8)$$

This empirical relation is used in Janningloring, wever to relate the starting time of transformation from isothermal and anisothermal. Pumphrey predicts the hardness of specimens after continuous and step-wise cooling

Different criteria and conditions have been proposed for the additivity of a transformation. Cahn and Avrami call it isokinetic when nucleation and growth rate are proportional at the same phase composition. The development of a phase at two different transformations is the same besides a time factor. In a logarithmic plot they look identical with the slower one shifted to the right side. directly quote Hollomon??

This equals to a condition

$$\dot{\beta} = g(\beta) h(T) \quad (2.9)$$

Cahn proposes a less strict condition

$$\dot{\beta} = f(\beta, T) \quad (2.10)$$

that is

It is shown in Lusk and Jou [1997] and Christian [2002] that this holds true for transformations that are isokinetic, c.f. Cahn [1956], and whose rate can be expressed in the following form

$$\dot{\beta} = h(\beta) g(T) \quad (2.11)$$

like eq. 2.6.

Based on the additivity rule Tzitzelkov et al. [1974] developed an algorithm to predict the phase development for continuous cooling. For this the cooling curve can be discretized into isothermal increments as in fig. 2.2.

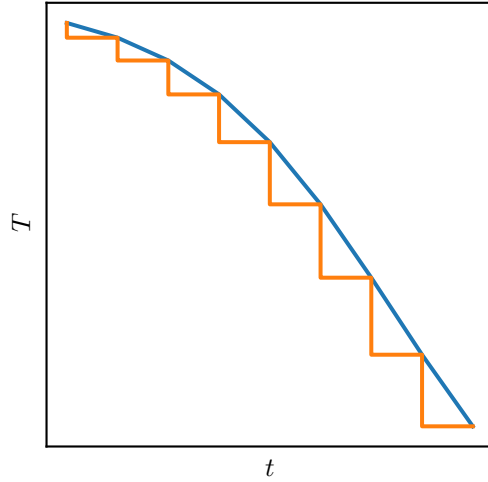


Figure 2.2: Continuous and incrementally isothermal discretized cooling curve.

The cooling curve is discretized into small isothermal steps at declining temperatures. Every step i is defined by its temperature T_i and its duration Δt_i .

In the following the procedure is explained using two isothermal steps of $\Delta t = 1.5s$ at the temperatures $T1 = 600^\circ C$ and $T2 = 550^\circ C$.

The first step starts at P0 with a volume fraction of bainite $\beta_B = 0$ and ends at P1 after Δt at $\beta_B^1 = 0.17$ following the transformation curve for T1. For the next step at T2, a fictitious point P1* is introduced. It is the intersection of $\beta_B = \beta_B^1$ with the transformation curve for T2. The time will be called fictitious time t^* . It is the time transformation at T2 would take to yield β_B^1 .

Then transformation is again following the curve for T2 for a Δt of 1.5s finishing at a volume fraction β_B of 0.78.

To incorporate the fictitious time into the rate equation the steps laid out in (Reti 2001) are done. Using the JMAK law 3.13, the fictitious time for a given volume fraction β_B and a temperature T the fictitious time t^* is derived as

$$t^* = \left(\frac{\ln A}{b(T_{i+1})} \right)^{\frac{1}{N(T_{i+1})}}, \quad A = \frac{\hat{\beta}}{\hat{\beta} - \beta_i} \quad (2.12)$$

This relation then is inserted into the rate equation 2.6 to replace the isothermal trans-

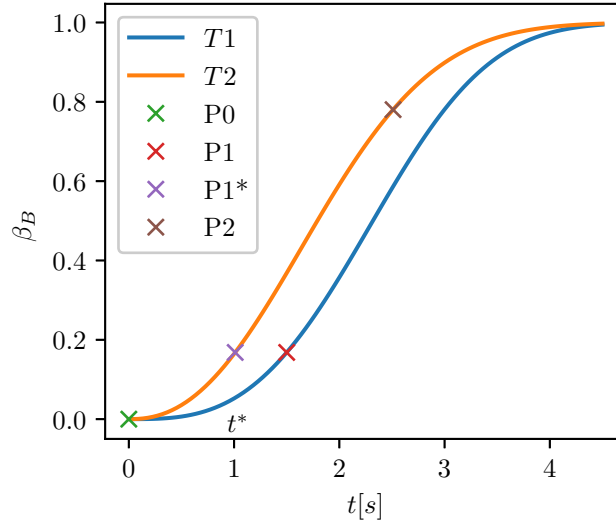


Figure 2.3: Two isothermal cooling steps.

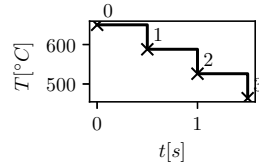


Figure 2.4: Discretized example cooling curve.

formation time and eliminate the explicit time dependence

$$\dot{\beta} = N b^{\frac{1}{N}} (\hat{\beta} - \beta) (\ln A)^{1 - \frac{1}{N}} . \quad (2.13)$$

The generalization of the rate equation for more phases *works similar* to the generalization of the martensitic rate. The maximal volume fraction of bainite $\hat{\beta}$ in (Oliviera 2010) is interpreted as

$$\hat{\beta} = \beta_A + \beta_B = 1 - \beta_M . \quad (2.14)$$

This leads to a desired coupling of the rate equations of Bainite and Martensite.

2.2.1 Involved Phases

Floris Osmond named Martensite after Adolf Martens in [Osmond \[1904\]](#)

2.2.2 phenomenological models

Kostinen Marburg

JMAK

Bringe ich die Metallurgie in dieses Kapitel und mische sie mit den Gleichungen oder trenne ich es in zwei Kapitel?

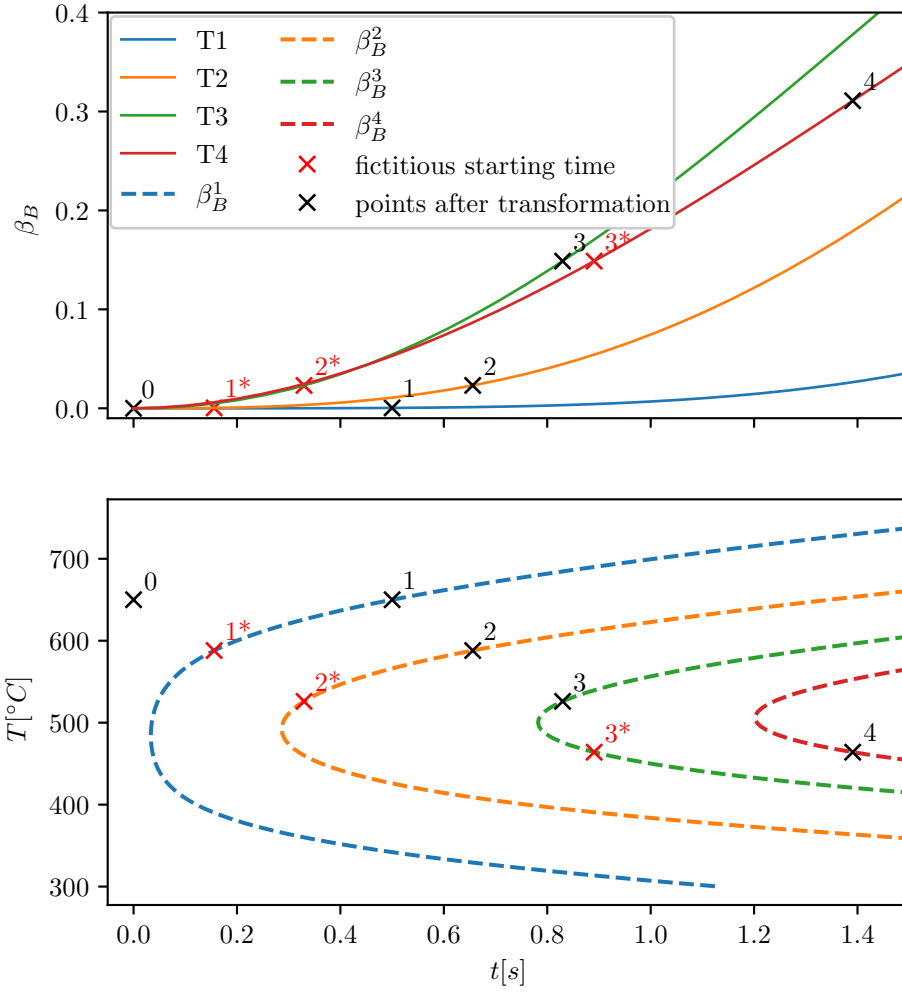


Figure 2.5:

2.3 Thermal Problem

The thermal problem is governed by the heat equation

2.4 mechanical

The heat treatment problem is solved for small strains. The strain measurement is defined as

$$\varepsilon = \frac{1}{2} (\nabla_x u + [\nabla_x u]') \quad (2.15)$$

with u being the displacement. The mechanical problem is governed by the balance of linear momentum

$$\nabla_x \sigma = 0 \quad . \quad (2.16)$$

The equations are now discretized and

Chapter 3

Algorithmic implementation

After establishing the rate equations for the phase transformations 2.13 and 2.3 in the previous chapter 2 there are modifications and regularisations necessary before one is able to use them for computation. For both equations a term ζ is introduced that controls whether transformation is happening or not, cf. Pacheco et al. [2001] and de Oliveira et al. [2010].

For the martensite transformation $\zeta_{A \rightarrow B}$ contains two heaviside functions Γ and a regularized step function using a tanh. The first heaviside function $\Gamma(-\Delta T)$ ensures irreversibility and that transformation only occurs during cooling. The second heaviside function $\Gamma(T - M_F)$ prevents transformation below the martensite finish temperature. The regularized step function $\tanh(A(M_S - T))/2 + 1/2$ starts the transformation after the temperature is below the martensite starting temperature. The regularization deals with the discontinuity of the transformation rate at $T = M_S$. The influence of A is depicted in fig. 3.1. The choice of $A = 1$ makes the effect of the regularization disappear

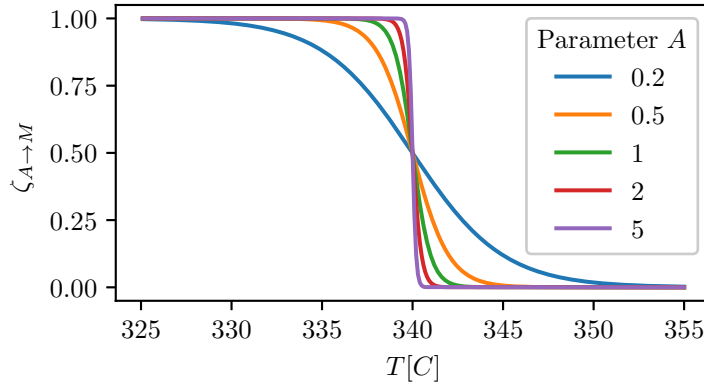


Figure 3.1: Regularized step function using a tanh with different parameters.

($< 1e - 6$) at $M_S \pm 2\%$.

This yields the extended rate equation for the evolution of the martensitic volume fraction

$$\dot{\beta}_M = -\zeta_{A \rightarrow M} \beta_A k \dot{T} \quad (3.1)$$

$$\text{with } \zeta_{A \rightarrow M} = \Gamma(-\Delta T) \Gamma(T - M_F) (\tanh(A(M_S - T))/2 + 1/2) \quad (3.2)$$

For the bainite transformation a new local time scale for every material point is

introduced. The transformation time τ starts once the temperature at the material point drops below the bainite starting temperature T_B^s . This time scale is used to account for vastly different incubation times at different temperatures. The incubation time is regarded as the time on the left of the bainite starting time t_B^s when looking at the TTT Diagram in fig. ??..

The time on the left of the bainite starting time t_B^s when looking at the TTT Diagram in fig. ??.. is regarded as incubation time. The incubation time τ necessary to start the transformation is vastly different at different temperatures. To account for this in a similar way to the anisothermal evolution of bainite, Scheill's additivity ?.. is used to determine when t_B^s is reached following a cooling curve.

The following condition is checked at every time step after an update of τ to determine the start of the transformation

$$\tau = \tau + \frac{\Delta T}{t_B^s} \quad (3.3)$$

$$t_B^s \geq \tau \quad . \quad (3.4)$$

The initial value problem represented by the rate equations is solved by implicit time integration which leads to the evolution equation $\beta^{n+1} = \beta^n + \Delta\beta^{n+1}$, with $\Delta\beta^{n+1} = \Delta t \dot{\beta}^{n+1}$.

After bringing these equations into residual form

$$\begin{aligned} \underline{\mathbf{R}}_\beta &= \underline{\beta}^{n+1} - \underline{\beta}^n - \underline{\Delta\beta} \\ &= \begin{bmatrix} R_{\beta_B} \\ R_{\beta_M} \end{bmatrix} = \begin{bmatrix} \beta_B^{n+1} - \beta_B^n - \Delta\beta_B^{n+1} \\ \beta_M^{n+1} - \beta_M^n - \Delta\beta_M^{n+1} \end{bmatrix} \end{aligned} \quad (3.5)$$

$$\text{with } \underline{\Delta\beta} = f(\underline{\beta}^{n+1}) \quad (3.6)$$

the backward Newton method is used to solve the equation system 3.5. The update of the backward Newton

$$\underline{\beta}^{k+1} = \underline{\beta}^k - \frac{\underline{\mathbf{R}}_\beta}{\underline{\mathbf{R}}_{\beta'}} \quad (3.7)$$

with the iteration counter k requires the derivation of the tangent

$$\underline{\mathbf{R}}_{\beta'} = \begin{bmatrix} \frac{\partial R_{\beta_B}}{\partial \beta_B} & \frac{\partial R_{\beta_B}}{\partial \beta_M} \\ \frac{\partial R_{\beta_M}}{\partial \beta_B} & \frac{\partial R_{\beta_M}}{\partial \beta_M} \end{bmatrix} \text{ with} \quad (3.8)$$

$$\frac{\partial R_{\beta_B}}{\partial \beta_B} = 1 - \Delta t b^{\frac{1}{N}} N \left[B^{1-\frac{1}{N}} - \left(1 - \frac{1}{N}\right) B^{-\frac{1}{N}} \right] \quad (3.9)$$

$$\frac{\partial R_{\beta_B}}{\partial \beta_M} = -\Delta t b^{\frac{1}{N}} N \left[B^{1-\frac{1}{N}} - \left(1 - \frac{1}{N}\right) B^{-\frac{1}{N}} \left(1 - \frac{\beta_A}{1 - \beta_M}\right) \right] \quad (3.10)$$

$$\frac{\partial R_{\beta_M}}{\partial \beta_B} = -k \Delta T \zeta_{A \rightarrow M} \quad (3.11)$$

$$\frac{\partial R_{\beta_M}}{\partial \beta_M} = 1 - k \Delta T \zeta_{A \rightarrow M} \quad . \quad (3.12)$$

3.1 Implementation in Abaqus

3.2 Avrami+addi

The equation used to describe this transformation is the JMAK law developed by [Johnson and Mehl \[1939\]](#), [Avrami \[1940\]](#) and Kolmogorov. It is only valid for isothermal transformations. The JMAK law

$$\beta = \hat{\beta} [1 - e^{-b(t^N)}] \quad (3.13)$$

can be used for various diffusional transformations and other time dependent processes from the crystallization of plastics [Cebe \[1988\]](#) to the growth of untreated tumors [Villar Goris et al. \[2020\]](#).

It yields sigmoidal shapes seen in [fig. 2.3](#) with a slow start and a slow finish of the transformation but a high rate in between.

To model nonisothermal transformation usually it is tried to relate it to the isothermal case and discretize a continuous cooling curve into isothermal steps and use the assumption of additivity. A different approach using two rates for nucleation and growth has been proposed in [Fasano et al. \[1991\]](#).

In [Scheil \[1935\]](#) a theory of the additivity of fractional nucleation is proposed to predict the start of the decomposition of austenite during cooling. The so-called ‘additivity rule’ states that transformation starts when the fractions of nucleation $\frac{\Delta t_i}{\tau(T_i)}$ accumulated during the cooling reaches unity

$$\int_{T_0}^{T_x} \frac{dt}{\tau(T)} = 1 \quad . \quad (3.14)$$

T_0 is an equilibrium temperature at which no nucleation happens, T_x is the temperature at which the transformation starts when following the nonisothermal temperature path and $\tau(T)$ is the incubation time after that transformation starts for an isothermal temperature path.

In the literature different conditions for the applicability of the additivity rule have been proposed. According to Avrami only isokinetic reactions are additive. For reactions described as isokinetic there is a constant ratio between the nucleation rate and the growth rate. In Avrami’s sense this is true for reactions with a constant N -value in the JMAK-law [eq. 3.13](#). Proof can be found in [Agarwal and Brimacombe \[1981\]](#).

Woher kommen auf einmal Nukleation und Wachstum

[Cahn \[1956\]](#) extended it to what he called general isokinetic transformations. In Cahn’s sense general isokinetic transformations are defined by a rate of the form

$$\dot{\beta} = g(T) h(\beta) \quad (3.15)$$

that can be written as two independent functions of T and β which are linked multiplicatively and is independent of the cooling rate \dot{T} .

In [Todinov \[1998\]](#) it is proven that [eq. 3.15](#) is a necessary and sufficient condition for the application of Scheil’s additivity in [eq. 3.14](#).

Cahn further broadened the valid application of additivity to any kinetic and cooling rate-independent transformations with a rate depending of T and β

$$\dot{\beta} = f(T, \beta) \quad . \quad (3.16)$$

This conclusion invalidated in [Lusk and Jou \[1997\]](#) by showing a class of transformation rates that is not additive in Scheil's sense. However [Agarwal and Brimacombe \[1981\]](#) proposes a numerical procedure for transformations that are not additive in accordance with eq. 3.14 but in a general sense when an nonisothermal path is approximated by isothermal steps.

The additivity rule has been used e.g. to predict hardness after transformation [Pumphrey and Jones \[1948\]](#) or to determine CCT-diagrams from TTT-diagrams [Tzitzelkov et al. \[1974\]](#).....

Now describe the algorithm of Agarwal and Reti/Cetinel) with fictitious time, nice graphs and stuff

3.3 Parametrisation of TTT-diagrams

For the procedures detailed in chapter ?? it is essential to determine the functions $N(T)$ and $b(T)$. They can be derived from TTT-diagrams as proposed in [Tzitzelkov et al. \[1974\]](#) ****Gefällt mir nicht****.

Time-Temperature Transformation (TTT) or Isothermal Transformation (IT) diagrams were first introduced in a study now considered as groundbreaking by [Davenport and Bain \[1930\]](#). They describe the decomposition of austenite into different phases at constant temperatures. In the following years after the mentioned study a large number of steels characterized in research papers and by steelmakers (c.f. [Vander Voort \[1991\]](#), [US Steel \[1963\]](#)).

To ****make them**** specimens are rapidly quenched to the ****zur untersuchenden**** temperature and held isothermally to investigate the transformation over time with the use of microscopy and dilatometry. In more recent years the usage of X-ray diffraction and transmission electron microscopy has become common.

The starting and the finish time of the transformation defined by a volume fraction of the product phase of 1 % and 99 % are entered into the diagram. This leads to the C-shapes seen in fig. ?? It is also common to see intermediate volume fractions of e.g. 10%, 50% and 90%. Nowadays the use of more advanced techniques like X-ray diffraction and transmission electron microscopy is common.

For the modelling of the phase transformations the parameters $N(T)$ and $b(T)$ need to be ...

The C-shaped lines of constant volume fractions β can be described by rearranging the JMAK law (eq. 3.13)

$$t^*(\beta, N(T), b(T)) = \frac{-\log(1 - \beta)^{1/N(T)}}{b(T)} \quad (3.17)$$

with the parameters $N(T)$ and $b(T)$ as functions of T.

Data points for the described lines and volume fractions of 1, 10, 50, 90 and 99 % are extracted from the IT-diagram for SAE 4140 provided in [Vander Voort \[1991\]](#) by using the Webplotdigitizer Tool by [Rohatgi \[2022\]](#).

By minimizing a cost function f for every temperature T_j

$$t^*(\beta, N, b) = \frac{-\log(1 - \beta)^{1/N}}{b} \quad (3.18)$$

$$f_j = \sum_i [t^*(\beta_i, N_j, b_j) - t(\beta_i, T_j)]^2 \quad (3.19)$$

$$N_j, b_j = \arg \min_{t^*} (f_j) \quad (3.20)$$

with the data points from the bainite region for $t^*(\beta_i, T)$ and $\beta_i = \{0.01, 0.1, 0.5, 0.9, 0.99\}$ N_j and b_j are determined for every T_j and plotted against the temperature in 3.2. For b it seems appropriate to use an exponential ansatz function so $\log b$ is also depicted. The sawtooth-like profile on the right side of each graph is the result of the decreasing number of data points per temperature at higher temperatures.

In [Yu \[1977\]](#) a second order polynomial ansatz is chosen for the parametrization of $N(T)$ and $\log b(T)$ while [Tzitzelkov et al. \[1974\]](#) uses a similar ansatz with polynomials of third order leading to the following parametrization

$$N = a + bT + cT^2 + dT^3 \quad (3.21)$$

$$b = \exp(e + fT + gT^2 + hT^3) \Leftrightarrow \log b = e + fT + gT^2 + hT^3 \quad . \quad (3.22)$$

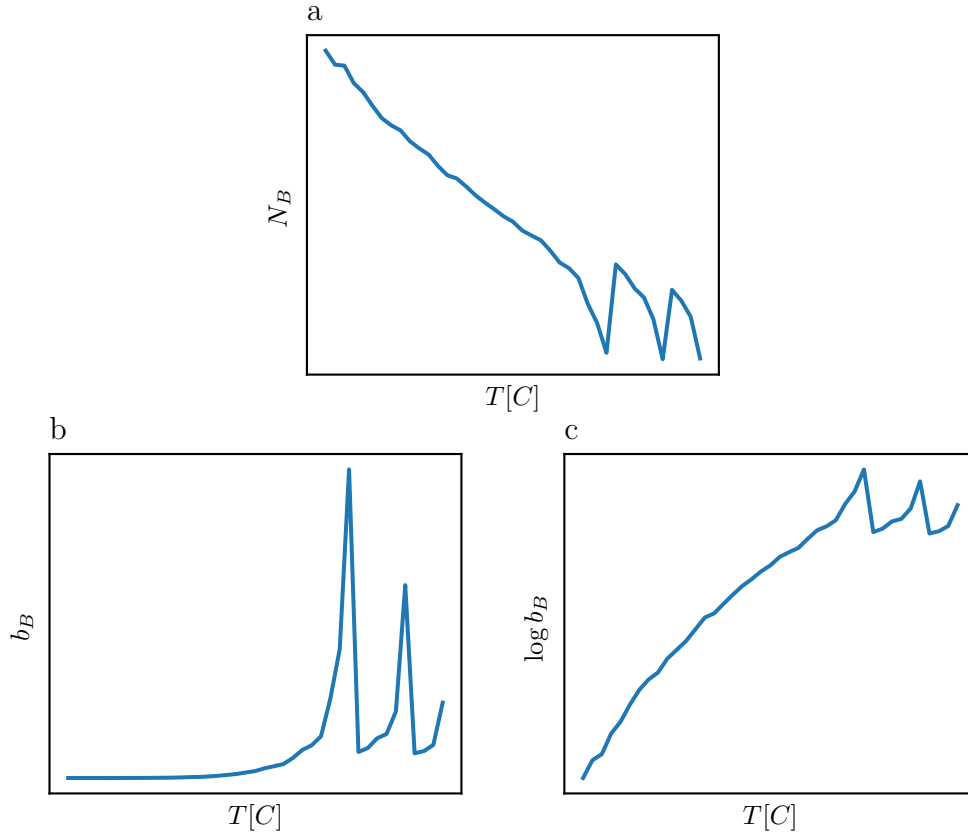


Figure 3.2: Parameters fitted from TTT-diagram.

Using a least square functional the

$$f = \frac{1}{2} \sum_i w_{8_i} [\log_{10}(t^*(\beta_i, N(T), b(T))) - \log_{10}(t(\beta_i, T))]^2 \quad (3.23)$$

with weights w_{8_i} assigned to C-shaped lines of constant β_i the coefficients of different polynomial ansatz for the bainite transformation are determined. The resulting TTT-diagrams are depicted in fig. ?? It is suggested to use the \log_{10} of the times to deal with data in a similar order of magnitude.

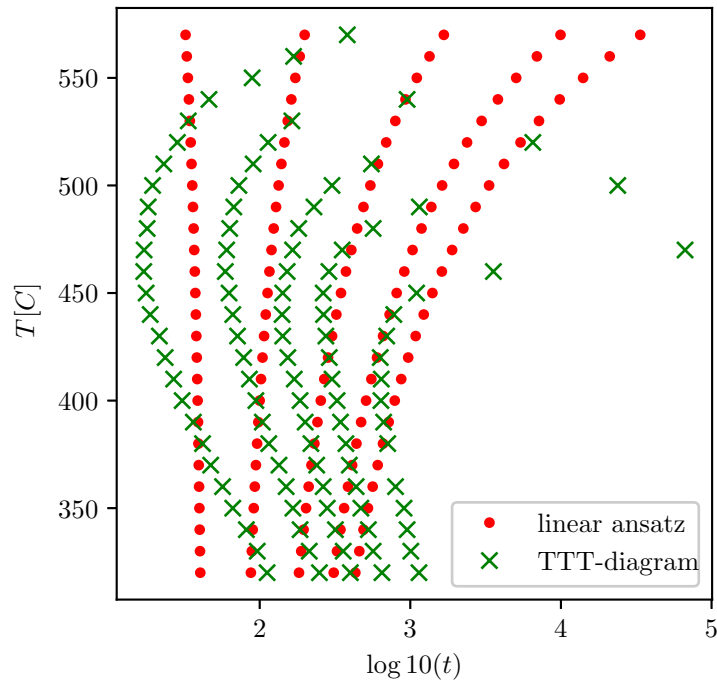
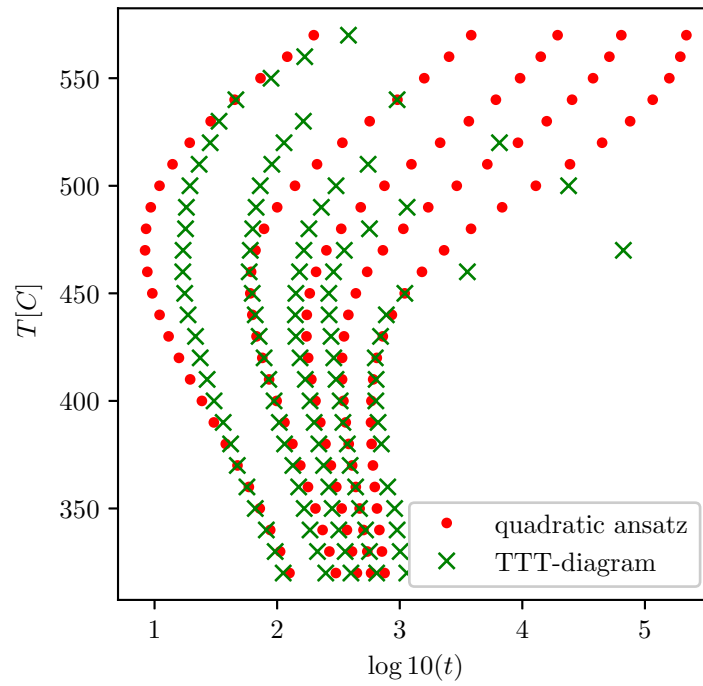
For SAE 4140 the use of polynomials of ... order seems appropriate which yields the following parametrization for the transformation into bainite

$$N = a + bT + cT^2 + dT^3 \quad (3.24)$$

$$b = \exp(e + fT + gT^2 + hT^3) \quad (3.25)$$

$$a = \dots \quad (3.26)$$

The dazugehörige TTT-diagram is depicted in fig. ??...

Figure 3.3: TTT-diagram with a linear polynomial ansatz for $N(T)$ and $\log b(T)$ Figure 3.4: TTT-diagram with a quadratic polynomial ansatz for $N(T)$ and $\log b(T)$

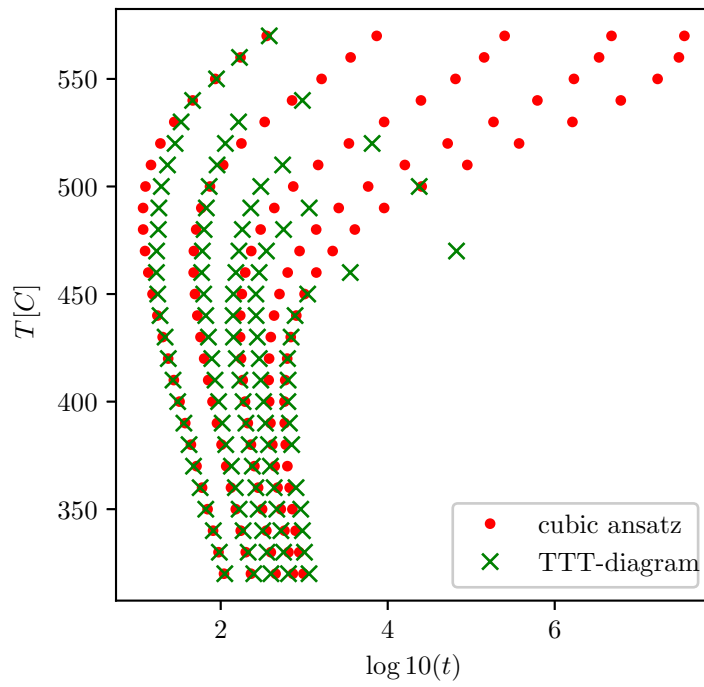


Figure 3.5: TTT-diagram with a cubic polynomial ansatz for $N(T)$ and $\log b(T)$

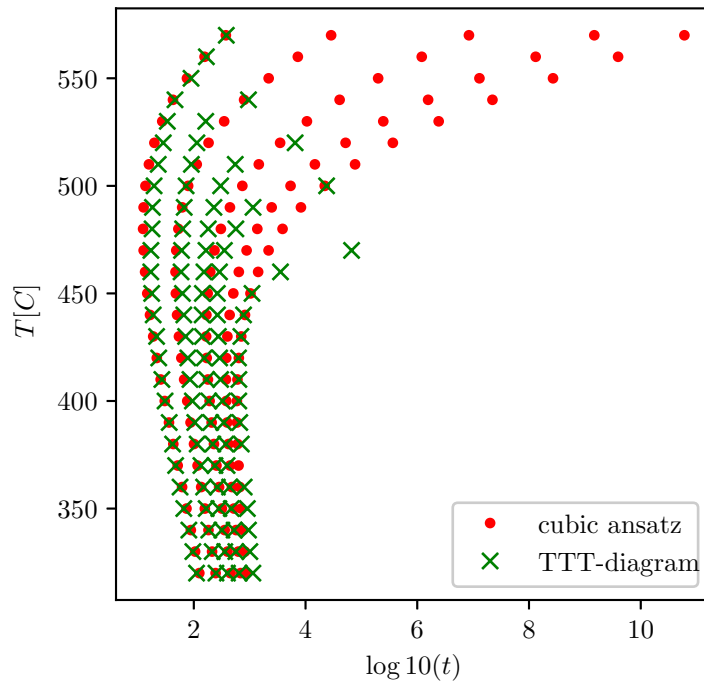


Figure 3.6: TTT-diagram with a cubic polynomial ansatz for $N(T)$ and a quadratic for $\log b(T)$

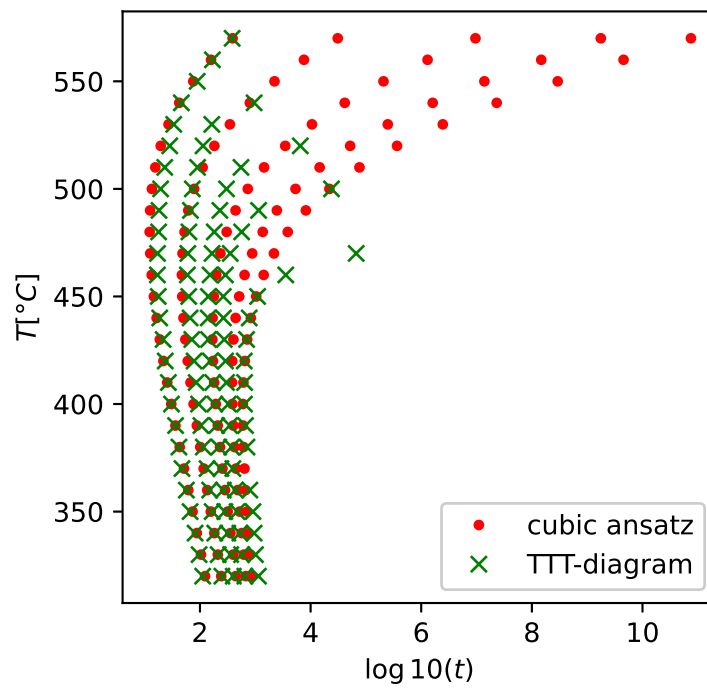


Figure 3.7: TTT-diagram with a quadratic polynomial ansatz for $N(T)$ and a cubic for $\log b(T)$

Bibliography

- Agarwal, P. K. and Brimacombe, J. K. (1981). Mathematical model of heat flow and austenite-pearlite transformation in eutectoid carbon steel rods for wire. *Metallurgical Transactions B*, 12(1):121–133.
- Avrami, M. (1940). Kinetics of Phase Change. II Transformation-Time Relations for Random Distribution of Nuclei. *The Journal of Chemical Physics*, 8(2):212–224.
- Bhadeshia, H. K. (2001). *Worked examples in the geometry of crystals*. Institute of Metals, London, 2nd edition.
- Bhadeshia, H. K. D. H. (2019). *Bainite in Steels: Theory and Practice*. CRC Press, 3 edition.
- Bhadeshia, H. K. D. H. and Christian, J. W. (1990). Bainite in Steels. *Metallurgical Transactions A*, 21(3):767–797.
- Cahn, J. W. (1956). Transformation kinetics during continuous cooling. *Acta Metallurgica*, 4(6):572–575.
- Cebe, P. (1988). Application of the parallel Avrami model to crystallization of poly(etheretherketone). *Polymer Engineering and Science*, 28(18):1192–1197.
- Christian, J. W. (1990). Simple geometry and crystallography applied to ferrous bainites. *Metallurgical Transactions A*, 21(3):799–803.
- Christian, J. W. (2002). Formal Theory of Transformation Kinetics. In *The Theory of Transformations in Metals and Alloys*, pages 529–552. Elsevier.
- Cohen, M., Olsen, G. B., and Owen, W. S. (1992). Martensite : a tribute to Morris Cohen.
- Davenport, E. S. and Bain, E. C. (1930). Transformation of austenite at constant sub-critical temperatures. *Trans AIME Chicago Meeting 1930, reproduced in Metallurgical and Materials Transactions B 1970*, 1(12):3503–3530.
- de Oliveira, W. P., Savi, M. A., Pacheco, P. M. C. L., and de Souza, L. F. G. (2010). Thermomechanical analysis of steel cylinders quenching using a constitutive model with diffusional and non-diffusional phase transformations. *Mechanics of Materials*, 42(1):31–43. Number: 1.
- DIN EN 10020 (2000). DIN EN 10020:2000-07, Begriffsbestimmung für die Einteilung der Stähle; Deutsche Fassung EN_10020:2000. Technical report, Beuth Verlag GmbH.

- Fasano, A., Andreucci, D., and Primicerio, M. (1991). Modelling the Solidification of Polymers: An Example of an ECMI Cooperation. In O'Malley, R. E., editor, *Proceedings of the Second International Conference on Industrial and Applied Mathematics*, pages 99–118. SIAM.
- Johnson, W. A. and Mehl, R. F. (1939). Reaction Kinetics in Processes of Nucleation and Growth. *Transactions of the American Institute of Mining and Metallurgical Engineers, Iron and Steel Division*, 135:416–442.
- Koistinen, D. and Marburger, R. (1959). A general equation prescribing the extent of the austenite-martensite transformation in pure iron-carbon alloys and plain carbon steels. *Acta Metallurgica*, 7(1):59–60. Number: 1.
- Lusk, M. and Jou, H.-J. (1997). On the rule of additivity in phase transformation kinetics. *Metallurgical and Materials Transactions A*, 28(2):287–291.
- Osmond, F. (1904). *Microscopic Analysis of Metals*. Charles Griffin & Company, Limited, London.
- Pacheco, P. M. C. L., Savi, M. A., and Camarão, A. F. (2001). Analysis of residual stresses generated by progressive induction hardening of steel cylinders. *The Journal of Strain Analysis for Engineering Design*, 36(5):507–516. Number: 5.
- Paxton, H. W. and Redmond, J. D. (2007). IRON AND STEEL. In Eugene A. Avallone, Theodore Baumeister III, and Sadegh, A., editors, *Marks' Standard Handbook for Mechanical Engineers, Eleventh Edition*. McGraw-Hill Education, New York, revised edition edition.
- Pumphrey, W. and Jones, F. (1948). Inter-relation of Hardenability and Isothermal Transformation Data. *JOURNAL OF THE IRON AND STEEL INSTITUTE*, 159(2):137–144. Publisher: INST MATERIALS 1 CARLTON HOUSE TERRACE, LONDON SW1Y 5DB, ENGLAND.
- Rohatgi, A. (2022). Webplotdigitizer: Version 4.6.
- Scheil, E. (1935). Anlaufzeit der Austenitumwandlung. *Archiv für das Eisenhüttenwesen*, 8(12):565–567.
- Todinov, M. T. (1998). Alternative approach to the problem of additivity. *Metallurgical and Materials Transactions B*, 29(1):269–273.
- Totten, G. E., editor (2007). *Steel heat treatment handbook*. CRC, Taylor & Francis, Boca Raton.
- Tzitzelkov, I., Hougardy, H. P., and Rose, A. (1974). Mathematische Beschreibung des Zeit-Temperatur-Umwandlung-Schaubildes für isothermische Umwandlung und kontinuierliche Abkühlung. *Archiv für das Eisenhüttenwesen*, 45(8):525–532.
- US Steel (1963). *USS Atlas of Isothermal Transformation Diagrams*. US Steel Company, Pittsburgh, PA.
- Vander Voort, G. F., editor (1991). *Atlas of time-temperature diagrams for irons and steels*. Materials Data Series. ASM International, Metals Park, Ohio, USA.

- Villar Goris, N. A., Selva Castañeda, A. R., Ramirez-Torres, E. E., Bory Reyes, J., Randez, L., Bergues Cabrales, L. E., and Montijano, J. I. (2020). Correspondence between formulations of Avrami and Gompertz equations for untreated tumor growth kinetics. *Revista Mexicana de Física*, 66(5 Sept-Oct):632–636.
- Yu, H.-J. (1977). *Berechnung von Abkühlungs-Umwandlungs-, Schweiss-, sowie Verformungseigenheiten mit Hilfe der Methode der Finiten Elemente*. PhD thesis, Universität Karlsruhe, Karlsruhe.